

## Research Article

### Protein Microarrays on ITO Surfaces by a Direct Covalent Attachment Scheme

Hou Tee Ng, Aiping Fang, Liqun Huang, and Sam Fong Yau Li

*Langmuir*, **2002**, 18 (16), 6324-6329 • DOI: 10.1021/la0255828

Downloaded from <http://pubs.acs.org> on February 3, 2009

#### More About This Article

---

Additional resources and features associated with this article are available within the HTML version:

- Supporting Information
- Links to the 3 articles that cite this article, as of the time of this article download
- Access to high resolution figures
- Links to articles and content related to this article
- Copyright permission to reproduce figures and/or text from this article

[View the Full Text HTML](#)



**ACS Publications**  
High quality. High impact.

# Protein Microarrays on ITO Surfaces by a Direct Covalent Attachment Scheme

Hou Tee Ng,<sup>†,‡</sup> Aiping Fang,<sup>†</sup> Liqun Huang, and Sam Fong Yau Li\*

Department of Chemistry, National University of Singapore, 3 Science Drive 3, S117543, Singapore

Received January 26, 2002. In Final Form: May 6, 2002

We describe the use of an indium tin oxide (ITO) thin film on a solid support serving as an effective generic immobilization platform to achieve one-step direct covalent attachment of arrayed proteins with good reproducibility and uniformity. Potential functional analyses on these surfaces involving protein–protein and protein–ligand interactions have been demonstrated. We also show that the approach can be adapted, via a photolithography-derived microwell route, to produce high-density protein microarrays which typically could accommodate a significantly higher density while occupying a comparatively smaller footprint than that achievable using currently existing high-precision robotic microarrayer systems, suggesting its potential applications in simultaneous parallel biological assays.

## Introduction

The significant impact brought upon by completion of the genome-wide sequencing projects<sup>1,2</sup> and the advent of microarray technology<sup>3</sup> cannot be overemphasized. The ready availability of genetic sequence information has progressively shifted genome-based research and development efforts toward gene-function-oriented studies.<sup>3–6</sup> A number of advantages have contributed to investigating biological processes on the protein level. For example, analyses of biochemical and related activities on the protein level could likely provide a far more effective choice for elucidating gene function, since it is manifested by direct activity of its translated protein. In addition, prediction of protein dynamics, structures, and interactions could be made more achievable than using genetics and DNA approaches.<sup>7</sup>

To facilitate such analyses in a massively parallel fashion, techniques analogous to DNA microarray technology<sup>8–15</sup> have been developed to meet these objectives. Recent protein microarray techniques for the high-

throughput screening of biochemical activities, protein–protein, protein–DNA, protein–RNA, protein–ligand interactions, and so forth, have been reported by numerous research groups.<sup>3–16</sup> Common to these techniques, proteins are introduced (using either spotting or printing technologies) in a grid format onto suitably prepared substrates, which commonly include silylated microscopic glass slides, photolithographically prepared gel pads, and chemically derivatized silicon substrates. Typical to these approaches, substantial efforts involving multiple-step complex surface treatment chemistries<sup>17–19</sup> and extensive processing protocols have to be invested to obtain the chemically derivatized substrates for subsequent protein immobilization, preferably via covalent attachment. One of the typical approaches involves using, for instance, small organic molecules such as organo-functional silanes and bifunctional alkanethiols as the bridging mediators to facilitate attachment of proteins to the modified substrates. However, stringent process controls are typically required in order to obtain high-quality modified substrates. Strong emphasis is thus placed on the uniformity, efficiency, and reproducibility of the approaches to modify the entire platform for reliable attachment of proteins for various functional analyses. In fact, satisfactory fulfillments of these criteria constitute extremely crucial factors to the success of the entire analysis since they determine the efficacy of the interactions and influence the eventual signal strength during the detection. Therefore, careful and consistently controllable surface chemical treatment is essentially required.

In view of the extreme stringent requirements in the pre- and post-treatments,<sup>17–19</sup> which are often complex and time-consuming, alternative approaches to effectively achieve simple, direct, reliable, and high-uniformity immobilization are highly desirable. While investigating the spontaneous self-assemblies of biomolecules on various solid-state surfaces, we have found that inter-metallic oxides, in particular, indium tin oxide (ITO),<sup>20</sup> serve as a

\* To whom correspondence should be addressed. E-mail: chmlifys@nus.edu.sg. Tel/Fax: 65-8742681.

<sup>†</sup> These authors contributed equally to the present work.

<sup>‡</sup> Present address: SETI Institute, NASA Ames Research Center, Mail Stop N229-1, Moffett Field, CA 94035.

(1) International Human Genome Sequencing Consortium, *Nature* **2001**, *409*, 860.

(2) Venter, J. C., et al. *Science* **2001**, *291*, 1304.

(3) Lueking, A.; Horn, M.; Eickhoff, H.; Bussow, K.; Lehrach, H.; Walter, G. *Anal. Biochem.* **1999**, *270*, 103.

(4) Zong, Q.; Schummer, M.; Hood, L.; Morris, D. R. *Proc. Natl. Acad. Sci. U.S.A.* **1999**, *96*, 10632.

(5) Junaid, Z.; Sabatini, D. M. *Nature* **2001**, *411*, 107.

(6) Zhu, H.; Klemic, J. F.; Chang, S.; Bertone, P.; Casamayor, A.; Klemic, K. G.; Smith, D.; Gerstein, M.; Reed, M. A.; Snyder, M. *Nat. Genet.* **2000**, *26*, 283.

(7) Anderson, L.; Seilhamer, J. *Electrophoresis* **1997**, *18*, 533.

(8) Shoemaker, D. D., et al. *Nature* **2001**, *409*, 922.

(9) MacBeath, G.; Schreiber, S. L. *Science* **2000**, *289*, 1760.

(10) Taton, T. A.; Mirkin, C. A.; Letsinger, R. L. *Science* **2000**, *289*, 1757.

(11) Pollack, J. R.; Perou, C. M.; Alizadeh, A. A.; Eisen, M. B.; Pergamenschikov, A.; Williams, C. F.; Jeffrey, S. S.; Botstein, D.; Brown, P. O. *Nat. Genet.* **1999**, *23*, 41.

(12) Walt, D. R. *Science* **2000**, *287*, 451.

(13) Kononen, J. *Nat. Med.* **1998**, *4*, 844.

(14) Singh-Gasson, S. *Nat. Biotechnol.* **1999**, *17*, 974.

(15) Steemers, F. J.; Ferguson, J. A.; Walt, D. R. *Nat. Biotechnol.* **2000**, *18*, 91.

(16) Okamoto, T.; Suzuki, T.; Yamamoto, N. *Nat. Biotechnol.* **2000**, *18*, 438.

(17) Cass, T.; Liger, F. S. *Immobilized biomolecules in analysis: a practical approach*; Oxford University Press: New York, 1998.

(18) Wu, G.; Datar, R. H.; Hansen, K. M.; Thundat, T.; Cote, R. J.; Majumdar, A. *Nat. Biotechnol.* **2001**, *19*, 856.

(19) Halliwell, C. M.; Cass, A. E. G. *Anal. Chem.* **2001**, *11*, 2476.

(20) Fang, A.; Ng, H. T.; Li, S. F. Y. *Langmuir* **2001**, *17*, 4360.

promising candidate as a highly stable generic platform for achieving spontaneous direct attachment of a wide range of biomolecules and organic molecules possessing sterically accessible reactive carboxyl functional groups. Such an attachment scheme, when combined with currently existing well-established microarray spotting technologies, could likely present a widely applicable alternative approach that aims to do away with the tedious and laborious surface chemical pretreatments to fulfill eventual one-step direct intact covalent immobilization of proteins for functional analyses.

For the protein-ITO covalent attachment scheme to be useful in microarray applications for most functional assays, several criteria must be taken into consideration. First, such an immobilization must be stable, with each entity anchored firmly on the ITO surfaces. Indeed, we have found that proteins could be attached covalently, spontaneously, and robustly onto the ITO surfaces. Interfacial surface information as acquired from surface-sensitive techniques, for instance, attenuated total reflection Fourier transform infrared (ATR-FTIR) spectroscopy, on a wide range of biomolecules, including antibodies, antigens, enzymes, and so forth, has revealed formation of  $M^+COO^-$  (where  $M$  = indium or tin) covalent linkages (absorption bands between 1600 and 1400  $cm^{-1}$ ) between their carboxyl groups and the abundant reactive hydroxyl groups ( $\sim 12$ – $13$  OH groups per  $nm^2$ ) on the ITO surfaces, which act to increase the probability of the binding activities and hence enhance the uniformity and density of the one-step attachment process.<sup>17,20–23</sup> The existence of the carboxylate linkage was also verified by the inability to stably immobilize the ITO surfaces with a modified protein, in which its surface free carboxyl groups have been deactivated via a carbodiimide activation prior to immobilization.<sup>24</sup> Moreover, the absence of reduced signal intensity of the spotted proteins after the chemical surface quenching step involving a high concentration of bovine serum albumin (BSA) solution suggests further the covalent nature of the immobilization. Such covalent linkages with consequent self-assembly are found to be very spontaneous, typically approaching a near-to-complete monomolecular layered surface coverage within 15–20 min.<sup>21</sup> In fact, this is very crucial in most functional analysis since prolonged duration of incubation may lead to denaturation/deactivation of the biomolecules. On the basis of the results from monitoring the fluorescence intensity under the same excitation and imaging conditions of the confocal laser fluorescence scanner, no apparent leaching of FITC-tagged proteins from the ITO surfaces was observed when subjected to mechanical ultrasonication for even more than 10 min, suggesting the formation of strong covalent linkages between the immobilized proteins and the ITO surfaces. Nevertheless, other noncovalent interactions including hydrogen bonding and van der Waals interactions are believed to further enhance stabilization of the proteins on the ITO surfaces.<sup>21</sup>

Second, the native conformations and bioactivities of the proteins must be retained after the immobilization, with favorable molecular orientations since these significantly affect the accessibility of their active site(s) toward targeted substrates during the interaction processes.

In this article, we aim to demonstrate the use of an ITO thin film on a solid support serving as an effective generic

immobilization platform to achieve one-step direct covalent attachment of arrayed proteins with good reproducibility and uniformity. Simple functional protein-protein and protein-ligand interactions using well-established examples will be demonstrated to show the efficacy of the approach. We also show that the present immobilization scheme could be adapted to ultraviolet (UV) photolithographic derived microwell-integrated ITO slides to obtain high-density microarrays, which may show potential in the realization of massively parallel biological assays.

## Experimental Section

**Microarraying of Proteins.** We used a robotic microarrayer (PixSys 5550, Cartesian Technologies) equipped with micromachined pins to consistently deliver samples of  $\sim 1$  nL onto the ITO slides at designated locations. Typical circular spots with diameters ranging from about 150 to 250  $\mu m$  and with a minimum pitch of about 250  $\mu m$  could be routinely obtained. Alternatively, we have also used micromolded poly(dimethylsiloxane) (PDMS) slabs with arrays of through-holes (diameters of 300–500  $\mu m$ , periodic pitches of 0.5–1.0 mm, and thickness of  $\sim 500$   $\mu m$ ) serving as the physical barriers/wells and manually introduced the protein aliquots. Similar to most microarray spotting experiments, we initially encountered the problem of rapid dehydration of the spotted proteins. Thus, all protein solutions, unless otherwise stated, were prepared in phosphate-buffered saline (PBS, pH 7.4) with 40% glycerol added to circumvent dehydration<sup>4</sup> and ring-formation of the microspots. After spotting, the protein-immobilized slides were kept in a humidity chamber (64% relative humidity) at room temperature (RT) for 2 h. Although the self-assembly process is spontaneous and could be accomplished within  $\sim 15$ – $20$  min (without added glycerol), we have experimentally found an incubation time of 2 h to facilitate optimum immobilization with the added glycerol. After this time, the slides were carefully inverted and slowly dropped onto a PBS buffer (pH 7.4) containing 1.0% BSA (w/v) for 45 s, which slowly diffused the unbound proteins away from the slides. This was then followed by immersion of the slides into a newly prepared similar buffer for an hour at RT with gentle agitation, which spontaneously quenched the unreacted hydroxyl groups on the ITO surfaces and served effectively as a blocking agent to prevent binding of other proteins or chemical species in subsequent processing steps. Following a brief rinse with PBS buffer, the slides were ready for further processing.

**Functional Protein-Protein and Protein-Ligand Interactions.** All probing reagents, unless otherwise stated, were prepared to the desired concentrations using PBS buffer containing 1.0% BSA and 0.1% Triton X-100. For the antibody-antigen interactions, human (H) immunoglobulin (IgG), bovine (B) IgG, and chicken (C) IgG (reagent grade, Sigma) were first spotted and immobilized onto ITO slides according to the procedures mentioned earlier. After the blocking step with BSA, the slides were probed respectively with anti-HIgG-FITC (0.5  $\mu g/mL$ ) (whole molecule, ICN Biomedicals, Inc.), anti-BIgG-FITC (1.0  $\mu g/mL$ ), and anti-CIgG (1.0  $\mu g/mL$ ) (whole molecule, Sigma). After an hour of incubation/interaction at RT, the slides were first rinsed with PBS buffer, followed by immersion into a PBS buffer containing 0.1% Triton X-100 for 6 min with agitation. After a brief rinse with PBS buffer, the slides were ready for fluorescence scanning. For the protein A-antibody interactions, protein A-FITC (Sigma, 5.0  $\mu g/mL$ ) was used to probe the HIgG-, BIgG-, and CIgG-immobilized ITO slides and processed accordingly for scanning as described earlier. For the protein-ligand interactions, biotin-FITC (Sigma, 5.0  $\mu g/mL$ ) was used to probe the streptavidin (Sigma) immobilized ITO slides. For the high-density microarray involving microwell-integrated ITO slides, the microwells were filled with a biotin (Sigma, 0.5 mg/mL in HEPES at pH 7.0) solution to allow immobilization ( $\sim 30$  min) to take place and subsequently rinsed copiously with PBS buffer to wash away the unbound biotin molecules. This was then followed by probing with streptavidin-Cy3 (Sigma, 10.0  $\mu g/mL$  in 0.085 M  $NaH_2PO_4$  at pH 7.0) for  $\sim 30$  min and then rinsing copiously with PBS buffer. Scanning was performed after rapid stripping of the resist using a 1:1 methanol/water (v/v) mixture.

(21) Fang, A.; Ng, H. T.; Su, X.; Li, S. F. Y. *Langmuir* **2000**, *16*, 5221.

(22) Meyer, T. J., et al. *Inorg. Chem.* **1994**, *33*, 3952.

(23) Ulbrich, R.; Golfik, R.; Schellenberger, A. *Biotechnol. Bioeng.* **1991**, *37*, 280.

(24) Unpublished data.

**Integration of Microwells onto ITO Slides.** We first deposited a uniform thin layer of ITO ( $\sim 25$  nm) onto a commercially available glass slide ( $75$  mm  $\times$   $25$  mm  $\times$   $1.1$  mm; Erie Scientific Co., Portsmouth) using a magnetron sputtering system (Discovery-18; Denton Vacuum, Inc.). Alternatively, we have also used other sources of ITO and obtained comparatively good results. After ultrasonication ( $\sim 1$  h) of the ITO-coated slide in a methanol (HPLC grade) bath, spin-coating (2000 rpm; Cee 100 Spinner, Brewer Science Inc.) was then performed to introduce a uniform thin layer of photosensitive resist (Shipley microposit S1813, Shipley Co. Inc.). Slides with varying thickness ( $1$ – $5$   $\mu$ m) of the resist have been successfully employed for the assays. Upon preliminary curing at an elevated temperature ( $95$   $^{\circ}$ C for 30 min), the resist-coated slide was exposed selectively through a contact mask under UV irradiation (FIAR Speedplate Printing Down, Votra Pte. Ltd.). After appropriate wet chemical development of the exposed resist (Shipley microposit developer 351) and thorough rinsing with ultrapure water ( $18.2$  M $\Omega$   $\text{cm}^{-1}$ ), arrays of systematically aligned microwells could be observed under the optical and scanning electron microscopes. The microwell-integrated ITO slide could then be used for performing various functional analyses after heat treatment at  $\sim 110$   $^{\circ}$ C ( $\sim 15$  min) to get rid of the possible entrapped water residues.

**Laser-Induced Fluorescence Scanning and Data Analysis.** We used a confocal laser fluorescence scanner (ScanArray 5000, GSI Lumonics) to acquire the laser-induced fluorescence (LIF) images (at a resolution of  $5$   $\mu$ m, 85% photomultiplier tube (PMT) and 98% laser power) using two lasers to separately measure the FITC and Cy3 emissions. All images were false-colored accordingly and processed using Adobe Photoshop V6.0, unless otherwise stated. Analysis of the fluorescence intensity was performed using the QuantArray Microarray Analysis software (GSI Lumonics, USA) for respective 16 bit TIFF images.

## Results and Discussion

To demonstrate the technique's applicability for functional assays, we first investigated protein–protein interactions whereby the antibody–antigen interactions were taken as the examples. We first arrayed three antibodies, namely, HIgG, BIgG, and CIgG, in rows of 10 on the ITO slides and probed accordingly with their FITC-labeled polyclonal secondary antibodies.

As shown in Figure 1A–C, when each of the slides was individually probed with its respective secondary antibody and scanned under a laser fluorescence scanner, localized green fluorescent spots corresponding to locations of respective antibodies became visible. Since minimum cross-reactivities<sup>25,26</sup> between the different species were expected, neighboring consistently faint fluorescent spots were observed as well. However, when all the three secondary antibodies were used to probe the antibody-arrayed ITO slides simultaneously, we observed simultaneous fluorescence of all the spots (Figure 1D) with almost the same intensities corresponding to those shown in panels A–C. The consistently obtained results, as reflected by the uniformity in intensity and the almost circular geometry of the fluorescence images within each row and from repetitive experiments, indeed suggest high reliability and reproducibility of the present immobilization scheme, that is, immobilization of the IgGs for high-specificity bindings with their cognate counterparts. Detection of analytes in the pg/mL range has also been performed with satisfactory results (not shown) from complex solutions (e.g., cell lysates and sera), suggesting the technique's applicability in the protein microarray field.<sup>27</sup> We have also used the present approach to demonstrate protein–small molecule (ligand) interactions

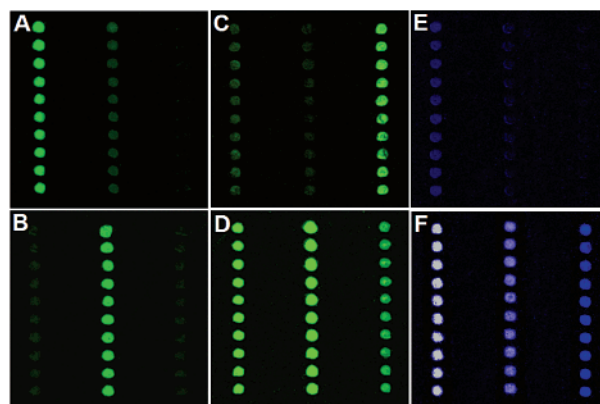


**Figure 1.** Spontaneous immobilization of proteins on ITO slides for functional protein–protein interactions. (A–C) LIF images of IgG-immobilized ITO slides probed with anti-HiGg–FITC ( $0.5$   $\mu$ g/mL), anti-BiGg–FITC ( $1.0$   $\mu$ g/mL), and anti-CiGg–FITC ( $1.0$   $\mu$ g/mL), respectively. (D) LIF image of an IgG-immobilized ITO slide probed simultaneously with all the secondary antibodies. (E) LIF image of an IgG-immobilized ITO slide probed with protein A–FITC ( $5.0$   $\mu$ g/mL). HIgG, BIgG, and CIgG were spotted in rows of 10 (starting from left to right) in all panels A–E. (F) LIF images of protein A immobilized ITO slides probed with HIgG–FITC of varying concentrations: (starting from left)  $20.0$ ,  $2.0$ , and  $0.2$   $\mu$ g/mL.

whereby the small vitamin biotin and the bacterial protein streptavidin were used<sup>26</sup> (not shown). The merits of the relatively fast turnover rate of the entire assays ( $\leq 4$ – $5$  h) should not be overlooked as well.

There are several other reasons that have also contributed to the usage of ITO as an ideal immobilization platform for protein microarrays. First, ITO could be prepared on a variety of potential substrates (suitable for microarray applications), including standard microscopic glass slides, silicon wafers, and various rigid polymeric sheets, as a high-quality uniform thin film using the well-established physical sputtering and evaporation techniques.<sup>29</sup> Promising results have also been obtained with these substrates. However, for the present microarray experiments, we have used the standard microscopic glass slides ( $75$  mm  $\times$   $25$  mm  $\times$   $1.1$  mm thickness) as the supporting substrates.

In addition, the consistent surface nanoroughness (root-mean-square (rms)  $\sim 1.19$  nm with associated fractal dimension,  $D$ ,  $\sim 2.13$ ) and surface morphology, which consists of nanocrystalline structures with grain sizes ranging from  $30$  to  $60$  nm as probed by scanning tunneling microscopy (STM), have allowed for good uniformity and high-density protein immobilization. For example, as shown by the STM nanographs in Figure 2B,C, HIgG molecules were observed to immobilize almost uniformly on the ITO surfaces, following the surface contours of the nanocrystalline grains to reveal an even finer grainlike morphology, presumably due to side-by-side aggregations of the HIgG molecules to form a self-assembled monomolecular layer. An estimated packing density of  $\sim 0.2 \times 10^{-11}$  mol  $\text{cm}^{-2}$  has been obtained while taking into consideration the surface roughness (root-mean-square  $\sim 2.77$  nm with associated fractal dimension,  $D$ ,  $\sim 2.17$ ). The latter has been further confirmed from ITO coated quartz crystal microbalance studies<sup>21</sup> which show a comparable surface coverage of  $\sim 1.0 \times 10^{-11}$  mol  $\text{cm}^{-2}$ .

(25) Diamandis, E. P.; Christopoulos, T. K. *Immunoassay*; Academic Press: San Diego, 1996.

(26) Harlow, E.; Lane, D. *Using antibodies: a laboratory manual*; Cold Spring Harbor Laboratory Press: New York, 1999.

(27) Manuscript in preparation.

(28) Diamandis, E. P.; Christopoulos, T. K. *Clin. Chem.* **1991**, *37*, 625.

(29) Schuegraf, K. K. *Handbook of thin-film deposition processes and techniques: principles, methods, equipment, and applications*; Noyes Publications: Park Ridge, NJ, 1988.

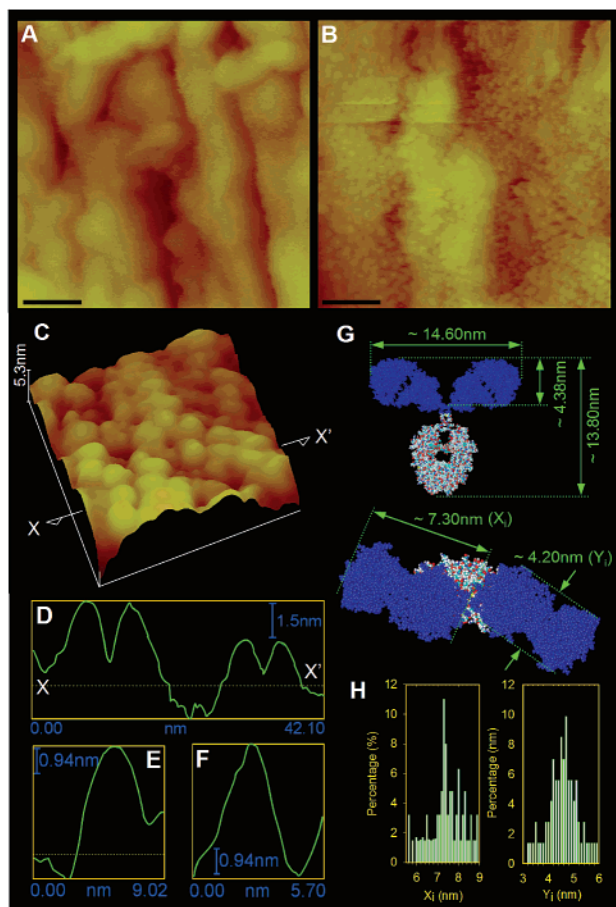


**Figure 2.** Surface morphology of HlgG molecules on an ITO surface. (A) A 2D STM nanograph (tunneling current, 180 pA; tip bias, 1.2 V; scan rate, 0.8 Hz) of the bare ITO, showing a nanocrystalline surface morphology composed of grainy structures with grain sizes ranging from about 30 to 60 nm (rms nanoroughness  $\sim 1.19$  nm with associated fractal dimension ( $D$ )  $\sim 2.13$ ). Scale bar, 50 nm; vertical  $z$ -height, 9.5 nm. (B) A 2D STM nanograph (tunneling current, 163 pA; tip bias, 5.0 V; scan rate, 0.5 Hz) showing the surface topography of HlgGs immobilized almost uniformly on the ITO surface, revealing a finer grainy morphology, presumably due to lateral or side-by-side aggregations of the HlgG molecules to form a self-assembled monomolecular layer (rms nanoroughness  $\sim 2.77$  nm with  $D \sim 2.17$ ). Scale bar, 50 nm; vertical  $z$ -height, 15.8 nm. (C) A zoom-in STM perspective view ( $41.5 \text{ nm} \times 41.5 \text{ nm}$ ) showing the globular nature of the immobilized HlgGs with noticeable double-loop pairings. Cross-sectional analyses of these surface features, as exemplified by  $XX'$  (as shown in D), E–F and statistically tabulated in H, show smooth convex contours with mean lateral displacements of  $7.33 \pm 0.94$  nm and  $4.43 \pm 0.60$  nm. (G) (top) A front view of a HlgG1 molecular model with highlighted (blue) Fab domains; (bottom) corresponding top view, which reveals the globular structures, analogous to that seen in the STM nanographs.

From the contour profiles of these surface globular features, mean lateral displacements of  $7.33 \pm 0.94$  nm and  $4.43 \pm 0.60$  nm have been calculated (Figure 2H), in good agreement with the physical structural dimensions ( $X_i$  and  $Y_i$ , respectively) of a human IgG1 molecular model.<sup>30</sup>

The good agreement between the experimentally obtained measurements and that of the molecular model and the fact that specific binding activities occur consistently could possibly suggest formation of direct covalent linkages likely to be through the sterically accessible

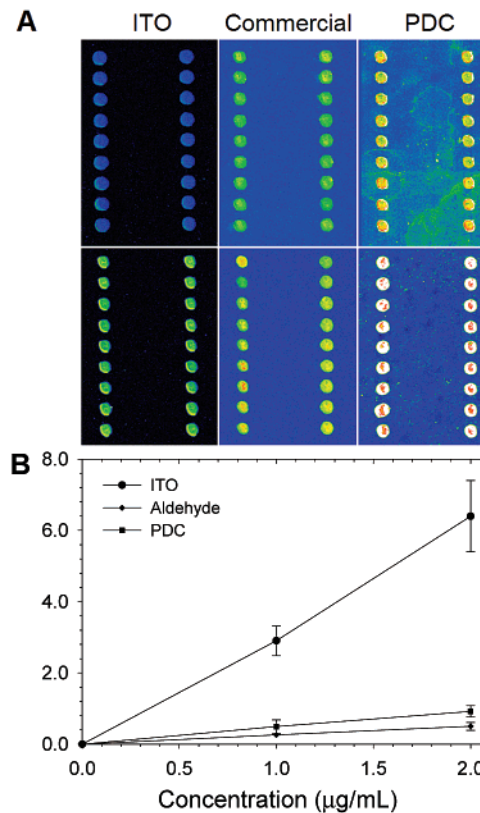


**Figure 3.** Direct side-by-side comparison of the performances of ITO, aldehyde (commercial), and PDC (ref 33) slides. (A) A series of LIF images of HlgG-immobilized slides probed with anti-HlgG–FITC (1.0 and 2.0  $\mu\text{g/mL}$  for top and bottom row panels, respectively). All images were acquired with the default rainbow-color setting and presented without image rendering. (B) A plot of  $\Delta F/F_0$  versus the concentration of the anti-HlgG–FITC probe for the three different microarray slides. As noted, the ITO slides provide the best signal-to-background ratio; with  $\Delta F/F_0$  exceeding that of the other two slides by at least twice.  $\Delta F = F_1 - F_0$ , where  $F_1$  is the measured fluorescence intensity of the microspot and  $F_0$  is the background fluorescence of the slides.

carboxyl groups (of glutamate (GLU)/aspartate (ASP) residues) from the heavy (H) chains of Fc domains of these glycoproteins and the hydroxyl groups on the ITO surfaces while maintaining favorable steric accessibility of the antigen binding sites of Fab domains of the antibodies to their cognate antigens (their polyclonal secondary antibodies in this case) in a self-assembly configuration. The latter could be indirectly and experimentally inferred when we subjected newly prepared antibody-arrayed ITO slides to protein A–FITC probes and vice versa. Since protein A, which is a 42-kDa protein from *Staphylococcus aureus*, is known to bind significantly stronger to the Fc domain of HlgG than to that of BIgG and to show absolutely no binding to CIgG,<sup>25</sup> the fluorescence pattern as shown in Figure 1E is thus anticipated. However, when compared to Figure 1F whereby HlgG–FITC was used as the probe, we observed a substantial variation in the intensity of the correlated signals with immobilized protein A. We observed higher fluorescence intensities even with a low probing concentration of HlgG–FITC (Figure 1F). This could be explained qualitatively by the increased steric hindrance of the Fc domains of the immobilized IgGs to the incoming protein A when one considers the structural covalent linkages as mentioned earlier. In contrast, such specific bindings should occur spontaneously in the latter case, hence leading to the observed increase in the binding activities (fluorescence signals).

(30) Clark, M. *Chem. Immunol.* **1997**, *65*, 88.

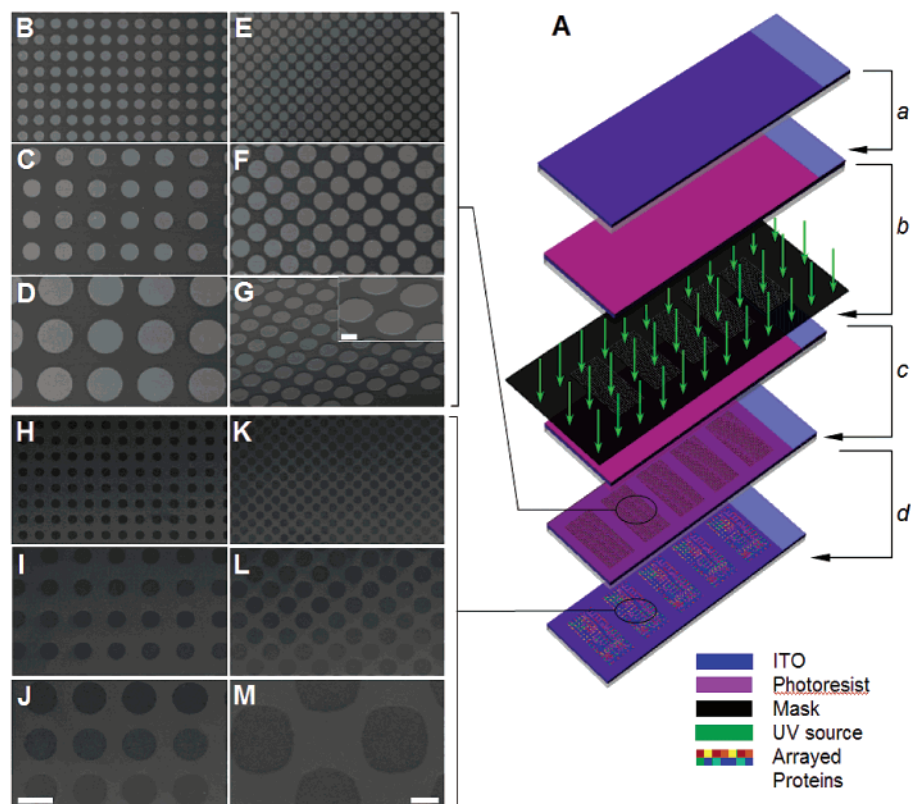


**Figure 4.** High-density integration of polymeric microwells on ITO slides. (A) A process flow illustrating the UV photolithographic approach of fabricating systematic arrays of microwells: (a) spin-coating of a uniform layer of UV-sensitive resist on a ITO slide; (b) selective exposure through a polymeric mask; (c) resist processing; (d) functional analysis followed by stripping of resist to reveal high-density arrays of biomolecular immobilized microspots. (B–G) A series of SEM images revealing consistently uniform microwells, having diameters ranging from 50 to 200  $\mu\text{m}$ , on the ITO slides obtained from the as-described approach. A perspective view of the microwells is shown in panel G, with an inset showing a zoom-in view of the microwells with  $\sim 2.5 \mu\text{m}$  thickness of the resist. The minimum lateral distance separation between the microwells attainable by the fabrication process is  $\sim 15 \mu\text{m}$ , limited essentially by the resolution of the image-setter used to fabricate the polymeric mask. (H–L) Corresponding SEM images showing excellent size matching and uniform arrays of immobilized biotin–streptavidin spots to that of the microwells in panels B–G after a resist-strip step. (M) Higher resolution view of (K). Scale bars: 200  $\mu\text{m}$  (for panels B–G, H–L), 50  $\mu\text{m}$  (for the inset of panel G), and 20  $\mu\text{m}$  (for panel M).

Besides, we have found ITO to provide a significantly better signal-to-noise ratio as it shows comparatively and significantly much lower background fluorescence than most chemically derivatized and commercially available aldehyde slides (see Figure 3). However, we found that a minimum film thickness of at least 10 nm is required to obtain the consistent low background fluorescence.

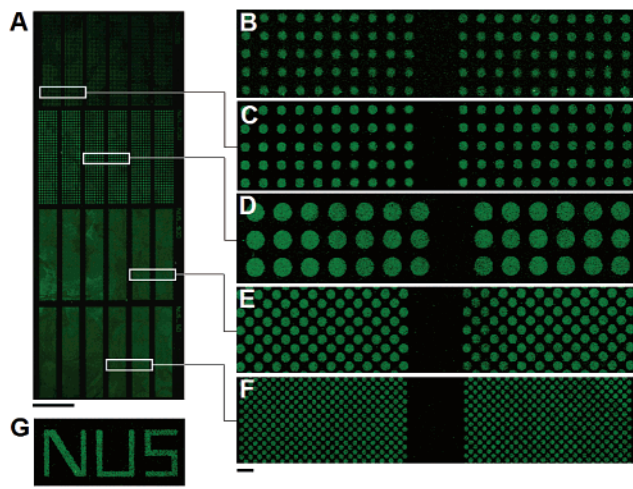
While it is beneficial that the present approach is compatible with current existing microarray technologies, it is equally important to look for effective means to increase the spotting density of the arrays so as to achieve high-throughput parallel analyses. We have taken advantage of the uniquely stable and highly processible nature of ITO and implemented the relatively straightforward UV photolithographic techniques<sup>31</sup> to reach our objective, that is, integration of high-density polymeric microwells onto the ITO slides.

Figure 4A depicts the process flow to obtain the desired arrays of systematically aligned microwells. As shown by the scanning electron microscopy (SEM) images in Figure 4B–G, uniform arrays of microwells with diameters and periodic pitches ranging from 50 to 200  $\mu\text{m}$  and from 90 to 280  $\mu\text{m}$ , respectively, could be routinely obtained. Array densities as high as 10579 and 21159 microwells per square centimeter could be achieved with the regular and hexagonal layouts, respectively.

To demonstrate its potential in functional interactions, we have employed the direct protein immobilization approach and the newly obtained microwell-integrated ITO slide to look into protein–ligand interaction studies, whereby the small vitamin biotin and the bacterial protein streptavidin were used as the examples.<sup>26</sup> Upon optimum immobilization, excess protein aliquots in the microwells were thoroughly rinsed away. When the FITC-labeled biotin was used to probe the streptavidin-arrayed ITO slides, distinct localized fluorescence corresponding to locations of the spotted streptavidin (microwells) was observed readily after removing the resist (Figure 5B). In fact, the same phenomenon was observed when we reversed their roles, that is, streptavidin–Cy3 conjugate was used to probe the immobilized biotin on the ITO slides (as shown in Figure 5A,C–G), but with slight dissimilar fluorescence intensities recorded in both situations (compare panels B and C of Figure 5). Indeed, we observed also noticeable nonuniformity in the two-dimensional (2D) fluorescence spots (especially along the circumference) in the former, which we attributed to possible steric hindrance of some immobilized streptavidin binding sites to the approaching biotin. Nevertheless, the observed results unequivocally suggest the unique advantages of both approaches to serve well in both protein function and protein-detecting microarrays.<sup>32</sup> Control experiments us-

(31) Chang, C. Y.; Sze, S. M. *ULSI Technology*; McGraw-Hill: New York, 1996.

(32) Kodadek, T. *Chem. Biol.* **2001**, *8*, 105.



**Figure 5.** Functional protein–ligand interactions on a microwell-integrated ITO slide. (A) A low-resolution LIF image, overviewing blocks of high-density biotin–streptavidin microarrays with a range of diameters and pitches achievable with the UV photolithographic approach. Streptavidin–FITC ( $10.0 \mu\text{g}/\text{mL}$ ) was used to probe the biotin-immobilized ITO slide. Scale bar, 5.0 mm. (B) A LIF image of a streptavidin-immobilized ITO slide probed with FITC–biotin ( $5.0 \mu\text{g}/\text{mL}$ ), for direct comparison with C. (C–F) Zoom-in LIF images corresponding to respective highlighted boxes in (A). Since the assaying conditions are essentially identical in each microwell, the high uniformity in the fluorescence intensity is thus anticipated. Scale bar,  $200 \mu\text{m}$ . (G) A LIF image of a “NUS” logo captured from the same ITO slide as shown in (A), showing the flexibility of the lithographic approach in creating customized patterns for functional assays. Scale bar,  $200 \mu\text{m}$ .

ing the same interaction pair on microwell-less ITO slides have also been performed and similar fluorescence in-

(33) Guo, Z.; Guilfoyle, R. A.; Thiel, A. J.; Wang, R.; Smith, L. M. *Nucleic Acids Res.* **1994**, *22*, 5456.

tensities were observed, suggesting the absence of significant artifacts that might occur as a result of unusual processing steps such as the stripping of the resist with 50% methanol. Similar results using the antibody–antigen pairs have also been obtained. Indeed, further extensions to various assays are possible using, for instance, a biotinylated molecule–(strept)avidin strategy for high-density parallel analyses.

There are several advantages of using the present immobilization scheme and microwell-integrated slides for functional assays. First, the individual interacting pairs of the substrates and the immobilized species are well separated and reside uniformly within each microwell, as can be seen from the SEM and fluorescence images (Figure 4H–M and Figure 5, respectively). An individual assay could be performed in a respective microwell with no cross-contamination, which could not be easily achieved with the conventional microwell-less approaches. Second, the microwell format on the ITO slide is fully compatible with existing standard microarrays and detection equipment, after implementing an additional alignment step. Either aligned capillaries or a robotic microarrayer could be used to spot a finite nanoliter volume of proteins into each individual microwell. Third, the density of the microwells on each slide could be varied accordingly to meet individual requirements since it is solely dependent on the designs of the low-cost polymeric masks and the resolution of the fluorescence scanner.

**Acknowledgment.** This research was supported by the National University of Singapore (NUS) and the National Science & Technology Board (NSTB), Singapore, through the Biosensor Focused Interest Group (BFIG). Fluorescence and scanning electron microscopy work was conducted at the Clinical & Research Center and the Electron Microscopy Unit, NUS, respectively.

LA0255828